Supramolecular Chemistry

DOI: 10.1002/ange.201402696

Harnessing the Liquid-Phase Exfoliation of Graphene Using Aliphatic Compounds: A Supramolecular Approach**

*Artur Ciesielski, Sébastien Haar, Mirella El Gemayel, Huafeng Yang, Joseph Clough, Georgian Melinte, Marco Gobbi, Emanuele Orgiu, Marco V. Nardi, Giovanni Ligorio, Vincenzo Palermo, Norbert Koch, Ovidiu Ersen, Cinzia Casiraghi, and Paolo Samorì**

Abstract: *The technological exploitation of the extraordinary properties of graphene relies on the ability to achieve full control over the production of a high-quality material and its processing by up-scalable approaches in order to fabricate large-area films with single-layer or a few atomic-layer thickness, which might be integrated in working devices. A simple method is reported for producing homogenous dispersions of unfunctionalized and non-oxidized graphene nanosheets in N-methyl-2-pyrrolidone (NMP) by using simple molecular modules, which act as dispersion-stabilizing compounds during the liquid-phase exfoliation (LPE) process, leading to an increase in the concentration of graphene in dispersions. The LPE-processed graphene dispersion was shown to be a conductive ink. This approach opens up new avenues for the technological applications of this graphene ink as low-cost electrodes and conducting nanocomposite for electronics.*

In the last decade graphene has emerged as an exciting material possessing unprecedented properties thereby holding potential to impact many areas of science and technology.[1] The extraordinary electronic, thermal, and mechanical properties of graphene make it a promising candidate for practical applications[2] in electronics,[3] sensing,[4] energy storage,[5] and conversion,[6] as well as in catalysis,[7] and biological labeling.[8] Graphene can be obtained in very-high-quality sheets produced in limited quantities by micromechanical cleavage,[9] chemical vapor growth,[10] annealing SiC substrates,[11] ball-milling of graphite,[12] building up graphene from molecular building blocks[13] (bottom-up) and as defective sheets by reducing graphene oxide.[14] Defect-free sheets can be produced by exfoliating graphite towards graphene (top-down).[15] In particular, graphite can be exfoliated in liquid environments by exploiting ultrasounds to extract individual layers. The liquid-phase exfoliation (LPE)[16] process generally involves three steps, that is, dispersion of graphite in a solvent, exfoliation, and purification. Exfoliation of graphene occurs because of the strong interactions between the solvent molecules and the graphitic basal planes, overcoming the energetic penalty for exfoliation and subsequent dispersion. It has been reported that solvents with surface tensions of about 30–40 $mJ\,m^{-2}$, such as *N*-methyl-2-pyrrolidone (NMP 40 $mJ\,m^{-2}$),[17] *ortho*-dichlorobenzene (*o*-DCB 37 $mJ\,m^{-2}$),[18] *N*,*N*-dimethylformamide (DMF 37.1 $mJ\,m^{-2}$),[19] or pentafluorobenzonitrile (PFBN 30 $mJ\,m^{-2}$)[20] are typically good candidates for graphene exfoliation.

The intercalation compounds of graphite were first reported in the 1840s.[21] A good understanding over their structures was obtained in early 1930s with the introduction of X-ray diffraction techniques. Despite the beginning of systematic studies on their physical properties in the late 1940s, only recently the research on graphite intercalation compounds has become a field of intense activity.[19,22] In this regard, it was shown that the exfoliation of graphite in a liquid media could be assisted by using organic molecules such as surfactants,[23] functionalized pyrenes,[24] diazaperopyrenium

[*] Dr. A. Ciesielski, S. Haar, Dr. M. El Gemayel, Dr. M. Gobbi, Dr. E. Orgiu, Prof. P. Samorì
ISIS & icFRC, Université de Strasbourg & CNRS
8 allée Gaspard Monge, 67083 Strasbourg (France)
E-mail: samori@unistra.fr
Homepage: http://www.nanochemistry.fr

H. Yang, J. Clough, Dr. C. Casiraghi
School of Chemistry, Oxford Road
University of Manchester, Manchester M13 9PL (UK)

Dr. M. V. Nardi, G. Ligorio, Prof. N. Koch
Humboldt-Universität zu Berlin
Institut für Physik & IRIS Adlershof
Brook-Taylor-Straße 6, 12489 Berlin (Germany)

Dr. V. Palermo
ISOF-CNR
via Gobetti 101, 40129 Bologna (Italy)

G. Melinte, Prof. O. Ersen
Institut de Physique et
Chimie des Matériaux de Strasbourg (IPCMS), UMR 7504
23, rue du Loess, 67037 Cedex 08 Strasbourg (France)

Prof. N. Koch
Helmholtz-Zentrum Berlin für Materialien und Energie GmbH
Bereich Solarenergieforschung
Albert-Einstein-Str. 15, 12489 Berlin (Germany)

[**] We thank Dr. Markus Döbbelin for performing preliminary experiments. This work was supported by the European Commission through the Marie-Curie ITN GENIUS (grant number PITN-GA-2010-264694), the Graphene Flagship (grant number GA-604391), the NMP-CP HYMEC (project number 263073), and the FET project UPGRADE (project number 309056), the ESF-EuroGRAPHENE project GOSPEL, the ANR through the LabEx project NIE and the International Center for Frontier Research in Chemistry (icFRC). We acknowledge Profs. M.-W. Hosseini and S. Ferlay (UdS) for the access to the thermogravimetric analyses. P. May is acknowledged for assistance with the Raman measurements.

Supporting information for this article is available on the WWW under http://dx.doi.org/10.1002/anie.201402696.

dications,[25] and biomolecules.[26] The organic molecules mainly act as a stabilizer by physisorption of their hydrophobic moieties on the graphene surfaces once graphite is exfoliated by sonication. The exfoliation of graphene in water is particularly challenging because of the hydrophobic nature of the sheets, but surfactants can solve this problem and help exfoliated sheets to remain suspended. However, the use of water as a media is not recommended for the exploitation of graphene in electronic devices because the presence of residual water molecules at the interface with dielectrics can enhance charge-trapping phenomena.[27] Thus, the use of organic solvents as an exfoliating media has to be explored. The exfoliation in an organic media could be promoted by adding a further organic molecule acting as dispersion-stabilizing agent during the exfoliation process.[16] In particular, only two examples were reported so far on the use of noncharged small organic molecules. Graphene dispersions were prepared in NMP with the aid of nonionic porphyrin molecules.[22c] Organic molecules such as, for example, 1,2-distearoyl-sn glycero-3-phosphoethanolamine-*N*-[methoxy (polyethyleneglycol)-5000] (DSPE-mPEG) were also used to stabilize graphene sheets at the end of the exfoliation process to inhibit the re-stacking of graphene sheets.[19] It has also been shown recently, that polymeric systems can have an impact on the exfoliation yield.[28]

Here we show that the concentration of defect-free, few-layer-thick (with about 30% single layers) graphene dispersions in NMP can be increased by addition of simple alkane molecules in the LPE process. The chosen dispersion-stabilizing compound needs to meet primarily two criteria: 1) its adsorption energy on graphene has to be larger than the adsorption of solvent molecules; 2) it needs to be very well soluble/miscible in/with organic media such as $CHCl_3$. We focused our attention on two simple molecular modules, that is, 1-phenyloctane and arachidic acid, the calculated adsorption energy on graphene of which is (-19.1 and -28.2 kcal mol^{-1}, respectively) much higher than the adsorption energy of NMP (-8.5 kcal mol^{-1}; see the Supporting Information for details), thus fulfilling with criterion (1). Additionally, to qualitatively test the affinities of both molecules for graphene surface we performed scanning tunneling microscopy (STM)[29] experiments at the solid–liquid interface, using highly oriented pyrolitic graphite (HOPG) as a substrate. Self-assembly of molecular building blocks capable of undergoing controlled self-assembly from solution at surfaces and interfaces relies on a subtle balance between molecule–molecule, molecule–substrate, molecule–solvent, and solvent–substrate interactions leading to the targeted 2D patterns.[30] In fact, alkanes and in particular carboxylic acids are one of the first molecules visualized with the submolecular resolution at the solid–liquid interface by STM.[31] Because of its simple structure, capability to form highly ordered architectures on graphite surface, as well as its low costs we decided to focus our attention on its C_{20} derivative, that is, arachidic acid. Noteworthy, it is well accepted in the STM community that 1-phenyloctane (typically used as a solvent in STM experiments) by itself doesn't form ordered monolayers (at room temperature) at the solution–HOPG interface. Although its adsorption energy on graphene is as high as -19.1 kcal mol^{-1}, the dynamic nature of the adsorption/desorption process of this small molecule on HOPG occurs on a time scale which is much faster than the scanning speed of a STM tip, hindering its visualization by STM.

The self-assembly of arachidic acid in 2D has been investigated by applying 4 μL drop of a (100 ± 2) μM solution on the freshly cleaved HOPG surface. Given that the solvent used for STM experiments has to be apolar (dielectric constant, $\varepsilon = 2$–4), STM measurements cannot be performed by using NMP as a liquid medium ($\varepsilon = 31$), thus 1-phenyloctane was chosen as a solvent. The STM current image in Figure 1 shows a monocrystalline lamellar structure. In this

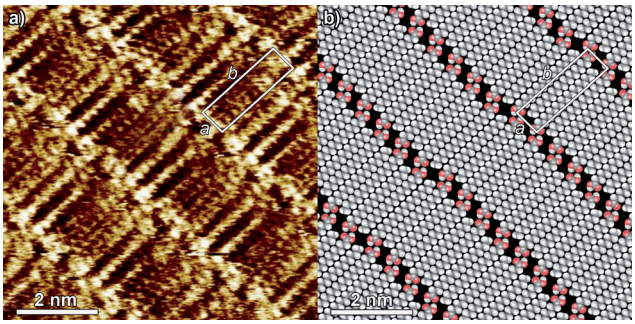

Figure 1. a) STM current image of arachidic acid monolayer at the HOPG–solution interface. b) Molecular packing motif. Tunneling parameters: average tunneling current (I_t) = 20 pA, tip bias voltage (V_t) = 350 mV. The scale bars are 2 nm.

2D crystal, arachidic acid molecules are physisorbed flat on the surface adopting an in-plane zig–zag conformation and forms H-bonded dimers, which are interdigitated between adjacent lamellae. Conversely, the 1-phenyloctane molecules have not been found to pack on HOPG. In light of this observation the calculated adsorption energy of arachidic acid on graphene is twice that of the monomeric species, thus amounting to -56.4 kcal mol^{-1}. The unit cell, containing two molecules, exhibits the following parameters: $a = (0.84 \pm 0.10)$ nm, $b = (2.52 \pm 0.10)$ nm, and $\alpha = (88 \pm 2)°$, leading to an area $A = (2.12 \pm 0.25)$ nm^2, in agreement with previous reports.[32]

To test the capability of the two molecules to increase the graphene exfoliation yields we prepared dispersions by adding graphite powder in NMP (1 wt%) by bath sonication (6 h), in the presence of the dispersion-stabilizing compounds, and compared it with the blank experiments, that is, a graphene dispersion prepared in the absence of additional molecules. By considering the initial graphite powder as a single graphene sheet, we calculated the number of molecules needed to form densely packed monolayers on graphene (see the Supporting Information). Given that the calculated quantity of the molecules will be higher than the real surface of graphite in the form of powder, we have used 5, 10, 15, and 20% of molecules needed to cover the entire graphene surface. Sonication of all samples, that is, two samples containing organic molecules and the one in their absence, led to gray liquids consisting of a homogeneous

phase and large numbers of macroscopic aggregates. As previously reported,[17a] these aggregates can be removed by centrifugation, yielding a homogeneous dark dispersion, which was also characterized by UV/Vis/IR absorption spectroscopy (see the Supporting Information for details).

To quantify the concentration after centrifugation, a mixture of graphene dispersion and $CHCl_3$ was heated at 50 °C and passed, through polytetrafluoroethylene (PTFE) membrane filters (pore size 100 nm). The remaining NMP solvent molecules were washed away with diethyl ether. The presence of adsorbed molecules on graphene sheets may affect the mass measurements and ultimately the exfoliation yields. Thus, we found that the heating process is necessary, in order to nearly completely remove, that is, desorb, the dispersion-stabilizing compounds from graphene (for details see the thermogravimetric analyses and X-ray photoelectron spectroscopic XPS analyses in the Supporting Information). Careful measurements of the filtered mass gave the concentration of dispersed phases after centrifugation (see Figure 2a).

The most significant increase of concentration was obtained by using 20% of molecules, where the graphene concentration amounts to 0.128 mg mL^{-1} and to 0.1 mg mL^{-1} for graphene exfoliated in the presence of arachidic acid and 1-phenyloctane, respectively. This corresponds to a nearly 50% increase in the yield of exfoliation if compared to samples prepared just in NMP (0.075 mg mL^{-1}). We decided to focus our attention on these three dispersions and analyzed them further.

UV/Vis/IR absorption spectroscopy gives the overall concentration of material dispersed in solution, but it does not provide information on the thickness composition of the material. Currently, the only method for identification of graphene produced by LPE is based on high-resolution transmission electron microscopy.[17a] Figure 2b shows our HR-TEM analysis: in a number of cases we observed folded monolayer graphene sheets with a size below 1 μm, as typically observed in LPE processed graphene.[15] The average lateral size of the monolayer graphene (MLG) sheets was nearly identical in all dispersions and amounts to (0.051 ± 0.012) μm^2. The number of layers per sheet was determined by analyzing the flake edges using HR-TEM (for HR-TEM images see the Supporting Information). Statistical analysis of the flake thickness is displayed in the histogram in Figure 2c: the percentage of single-layer graphene amounts to approximately 23% and 28% for NMP/arachidic acid and NMP/phenyloctane dispersion, respectively; NMP alone gives a single-layer percentage below 20%, showing that the aliphatic compounds improve the concentration of graphene.

Since the first successful exfoliation of graphene in an organic solvent such as NMP in 2008,[17a] improvements in concentrations of graphene dispersions were achieved, for example, through the addition of dispersion-stabilizing compounds such as nonionic porphyrin, obtaining concentrations as high as approximately 0.05 mg mL^{-1},[22c] or by using drastically longer sonication times (ca. 500 h-1.2 mg mL^{-1}). The latter approach is time consuming and requires high-energy consumption; in addition, it is known that with the increasing sonication time, the size of the flakes are severely reduced,[33] being a critical parameter for several applications. Therefore, a comparative study like the one presented here is extremely important to gain a deep understanding on the role of surface-stabilizing molecules in the graphene exfoliation process, which potentially can result in shortening and simplifying the LPE process. Noteworthy, we found that graphene dispersions prepared in the presence of arachidic acid molecules (0.12 mg mL^{-1}) are more concentrated if compared to samples prepared just in NMP (0.08 mg mL^{-1}), therefore corresponding to a 50% increase in the yield of exfoliation.

Although the formation of spatially extended, ordered, and stable self-assembled monolayer on graphene sheets during the sonication process is unlikely, the presence of the alkane molecules leads to an increased yield of exfoliation. As expected from different adsorption energies of phenyloctane and arachidic acid on graphene sheets, the latter exfoliates the graphene more effi-

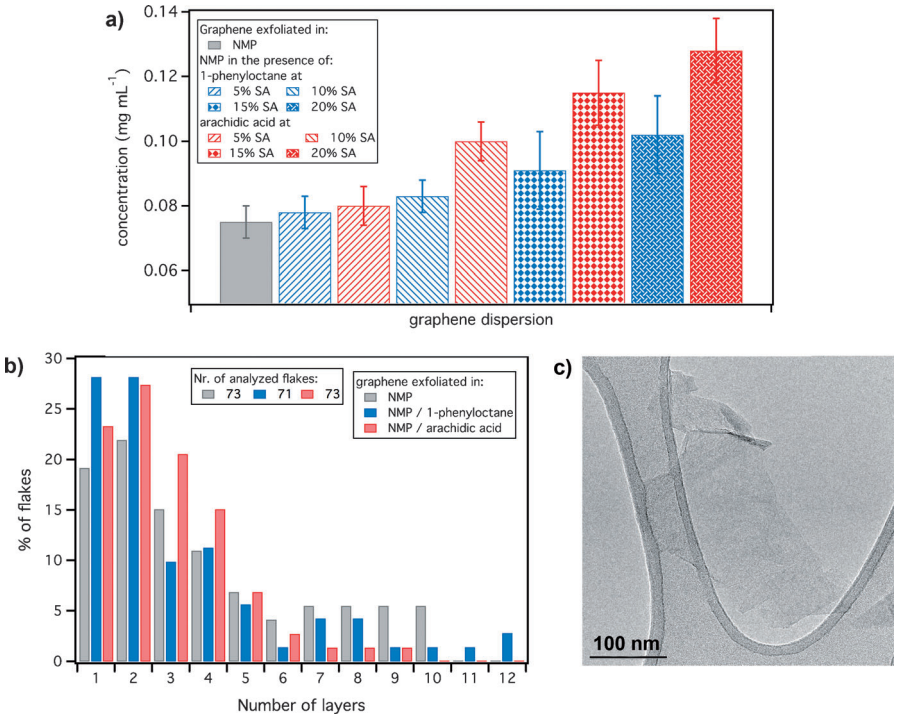

Figure 2. a) Average concentration of three dispersions after the filtration process. The error bars correspond to the statistical error obtained by averaging the data based on 15 independent experiments. b) Representative TEM image of graphene deposited from NMP dispersion showing folded graphene sheets. c) Histogram of the number of flakes observed as a function of number of layers per flake from NMP dispersions.

ciently, highlighting the importance of the molecular length in the structure of dispersion-stabilizing agents. In this regard, in order to explore the propensity of arachidic acid molecules to undergo dimerization in NMP, 2D ^{1}H NMR (DOSY) experiments have been carried out (see the Supporting Information). Surprisingly, diffusion coefficients provided evidence for the existence of monomeric species of arachidic acid in NMP. Although the majority of molecules exist as monomeric species in solution, it is likely that they undergo dimerization through H-bonding when the dimensionality is reduced from the three dimensions of a solution to the two dimensions on the graphene surface. This is in line with previous STM observations of H-bonded patterns obtained by dissolving molecules in similarly polar media like dimethylsulfoxide and further diluted with other solvents to form ordered monolayers at the solid–liquid interface, ultimately proving the key templating effect of the substrate.[34] Statistical analysis of the flake thickness revealed that the use of dispersion-stabilizing molecules increases the amount of produced graphene flakes, that is, increases the exfoliation yield, but also rises the percentage of mono- and bilayer graphene flakes produced in the LPE process.

We then focused our attention on comparing the quality of three graphene dispersions by the means of Raman spectroscopy, which is a powerful tool for the investigation of graphene.[35] We performed micro-Raman measurements by casting the suspensions on a silicon substrate, heated at 60 °C to facilitate NMP evaporation. In order to avoid damage and heating-induced effects, which can desorb or damage the molecules,[24d] the laser power was kept well below 1 mW. Note that the Raman spectrum of graphene produced by LPE is very different from the one of graphene produced by micromechanical exfoliation (MME).[36] This is expected since during sonication, the material is strongly interacting with the solvent and it is subjected to strong mechanical stress because of the collapse of bubbles and voids in the liquid, which ultimately break the flakes into smaller pieces: overall the process may produce considerable changes in the Raman peaks, which could be related to structural changes, but also doping, solvent residuals, and re-stacking.

Figure 3 shows the typical Raman spectra obtained from the NMP/aliphatic dispersions as compared to NMP-based dispersions. The first-order Raman spectrum of LPE graphene is characterized by the G and D peaks, at about 1580 and 1350 cm^{-1}, respectively. While the D peak is usually not visible in the Raman spectrum of MME graphene, this features is always observed in LPE graphene and it is attributed to its edges,[17a,37] which acts as "defects" in the Raman scattering process.[24d] Noteworthy, the D peak intensity increases with decreasing size of the flakes[17a] (typically smaller than the size of the laser beam) and it also depends on the excitation energy.[38] Therefore comparisons between different Raman spectra of LPE graphene should be done with care, and statistical analysis of intensities of both G and D peaks should be performed. For example, in our case, although the D peak in Figure 3 looks very strong, as compared to the G peak intensity, statistical analysis (see the Supporting Information) makes it possible to observe that for the NMP dispersions prepared in the presence of additional molecules the ratio between D and G peak intensities, I(D)/I(G), changes considerably from flake to flake (between 1 and 2.4). The average I(D)/I(G) ratio obtained for NMP dispersions is 1.6, showing that the dispersions are of comparable quality. This will be further confirmed by electrical measurements.

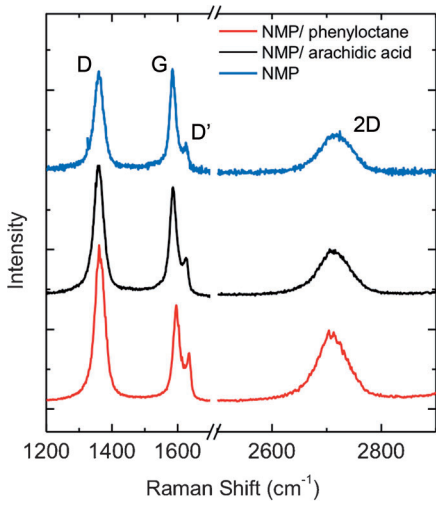

Figure 3. Typical Raman spectrum of graphene produced in NMP, NMP/arachidic acid, and NMP/phenyloctane. The single peak shape of the 2D peak indicates that ii is a single-layer flake.

The second-order Raman spectrum is very important because it allows qualitative identification of the thickness of the flakes through the 2D peak shape:[35b] in the case of MME graphene, a single layer has a single and intense peak, while few layers are composed by at least 2 broad components for AB stacking. However, in the case of graphene-based dispersions, the 2D peak can also assume complex lineshapes because of re-aggregation and folding. This can also affect the 2D peak intensity, making the Raman spectrum very different from the one of MME graphene.[17a] Therefore, one can only distinguish between three cases: single-layer flakes, AB thick flakes (i.e. graphite residuals), and thin flakes (with or without AB stacking). Thus, we compared the Raman spectra measured on 30–40 flakes of the dispersions obtained with and without the dispersing agent. While the first-order Raman spectra did not show strong differences, we observed a different 2D peak shape distribution between the dispersions: thick AB-stacked flakes have been rarely observed in the NMP/dispersing agent (either arachidic acid or phenyloctane), as compared to the NMP dispersion (see the Supporting Information). This provides unambiguous proof that the dispersing agent plays a key role in the exfoliation mechanism (that is in breaking the multilayered pieces of graphite), thereby increasing the overall yield. Furthermore, Raman spectroscopy shows that the addition of dispersion-stabilizing compounds does not affect the quality and structure of graphene, as compared to the use of NMP alone since there are no major changes in the first-order Raman spectrum (Figure 3). From the analysis on the 2D peak shape one can qualitatively estimate the thickness composition of the flakes in suspension: we found that overall

the percentage of single-layer graphene amounts to approximately 30% and 40% for NMP/arachidic acid and NMP/1-phenyloctane dispersion, respectively. The rest of the material is composed of thin flakes (< 10 layers), probably mostly re-aggregated MLG flakes, since AB stacking was never observed. This result is only qualitative as re-aggregation can happen after deposition of the material on the substrate. However, in first approximation, this analysis can be used for a first quantitative comparison between the quality and composition of different dispersions. In fact the results obtained by Raman spectroscopy are in good agreement with HR-TEM analysis (Figure 2).

To probe the electrical properties of the graphene exfoliated with and without dispersing agents, devices were prepared by drop-casting NMP dispersions onto dielectric substrates exposing pre-patterned interdigitated gold electrodes with variable channel length. Prior to the drop cast of graphene, the SiO_2 surfaces were treated with either hexamethylsilazane (HMDS) or octadecyltrichlorosilane (OTS) in order to evaluate the impact of the surface wettability on the electrical performances. The sheet resistance, R_s was extracted from the two-terminal I–V traces after taking into account the actual inter-electrode area coverage. The channel coverage, typically within 6 and 20% of the total area, was estimated by optical microscopy on each single device and the effective channel width of the electrodes (W) was consistently employed in the sheet resistance determination. The solutions were drop-casted as this deposition method is the closest to real ink-jet printing or roll-to-roll processes which allow mass production of large-area and low-cost electronics.

After the dispersion deposition on the test devices, a first set of measurements was recorded upon annealing samples at 45 °C for 2 days in order to get rid of residual solvent. However, the electrical characterization revealed high and inhomogeneous sheet resistance values which we ascribed to the presence of residual NMP in the film (see the Supporting Information for details). This intuition was experimentally verified by a 100-fold current increase upon annealing of the samples at 415 °C overnight (see the Supporting Information). Hence, the latter is a key step to gain a deep understanding on the transport properties, as the presence of residual NMP could be strongly detrimental for the conduction while not providing a reliable estimate of the electrical properties of the materials under test.

Figure 4 shows the lowest resistance measured in the 16 devices in every chip with different exfoliating agent and surface treatment. We found that the sheet resistance depends not only on the coverage but also on the concentration of the graphene flakes in the channel. When an OTS self-assembled monolayer was formed on silicon oxide, the drop-casted graphene solutions had greater tendency to sit on the gold electrodes resulting in a higher density of material between the electrodes when compared to the HMDS surface case, resulting in a typically lower average sheet resistance (see the Supporting Information for contact-angle measurements). The absolute values were found to fall in the 10–25 $k\Omega\,sq^{-1}$ range over several batches and are roughly 30-fold larger than in common CVD-grown graphene. This behavior is somehow expected if one considers that the injected charges undergo

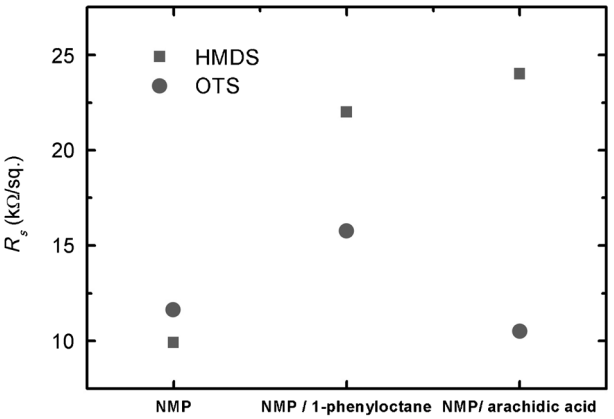

Figure 4. Comparative values of sheet resistance (R_s) for graphene with different exfoliating agents on octadecyltrichlorosilane (OTS) and hexamethylsilazane (HMDS) treated substrate. Plotted values represent the lowest measured resistance in the device in every chip. The values were corrected for coverage as the actual channel width (W_{eff}) was found to be lower than the nominal channel width of the electrodes (W).

flake-to-flake percolation in order to be collected at the other electrode. The flake-to-flake charge hopping could be clearly more detrimental for charge transport than in the case of a continuous layer with a few defects (CVD-graphene) where charges do not need to hop from a flake to another.

In addition, in order to quantify field-effect mobility the three different materials were characterized in Si-n^{++}/SiO_2 test patterns with the possibility of applying an additional (gate) voltage. Before the annealing at 415 °C, the FET devices showed ambipolar behavior with a clear Dirac point in the transfer curves (see the Supporting Information). After annealing at 415 °C, the graphene dispersion resulted p-doped with no clear Dirac point, which can be ascribed to the reappearance of the silanol groups after the annealing of the OTS and HMDS SAMs at such high temperatures. It has been widely reported that the Si-OH groups act as efficient electron traps.[27] In this case, the mobilities extracted from the transfer curves were found to range between 0.3 and 1 $cm^2\,V^{-1}\,s^{-1}$. These mobilities are in good agreement with those recently reported on devices integrating LPE-graphene deposited by a more cumbersome method such as Langmuir–Blodgett technique.[17b] We highlight that a much higher value for the mobility (above 100 $cm^2\,V^{-1}\,s^{-1}$) could be extracted from the linear conductance, as shown in detail in the Supporting Information. The I_{on}/I_{off} ratio was always found to be below 2, further indicating that LPE, likewise scotch-tape and CVD-grown graphene, could be best exploited to fabricate electrodes for electronics applications rather than acting as the active layer in FET devices.

We demonstrated that by mastering a supramolecular approach it is possible to improve the yield of graphene exfoliation in an up-scalable LPE-based method to produce high-quality graphene flakes from powdered graphite. By using a molecular module possessing high affinity for the graphite surface as dispersion-stabilizing agent, high-concentration dispersions of graphene were obtained. Our exfoliation protocol is effective: graphitic AB stack flakes were

rarely observed by Raman spectroscopy. Notably, the latter technique revealed that the addition of the simple alkane 1) does not affect the quality and structure of graphene, as compared to the use of NMP alone, highlighting the non-invasive nature of our procedure, and 2) leads to an increase the percentage of mono- and bilayer graphene flakes. In particular, by using 1-phenyloctane as dispersion-stabilizing agent the amount of MLG increases by ca. 10% and graphene concentration increases of 25%, with respect to graphene exfoliated in pure NMP. Conversely the addition of arachidic acid resulted in slightly lower increase of percentage of MLG and 50% increase of concentration. The LPE processed graphene dispersion was shown to be a conductive ink. Our approach opens up new avenues for the technological applications of graphene ink as low-cost electrodes and conducting nanocomposite for electronics.

Received: February 22, 2014
Revised: May 7, 2014
Published online: July 15, 2014

Keywords: electroactive materials · graphene · liquid-phase exfoliation · supramolecular chemistry

[1] K. S. Novoselov, A. K. Geim, S. V. Morozov, D. Jiang, Y. Zhang, S. V. Dubonos, I. V. Grigorieva, A. A. Firsov, *Science* **2004**, *306*, 666 – 669.
[2] K. S. Novoselov, V. I. Fal′ko, L. Colombo, P. R. Gellert, M. G. Schwab, K. Kim, *Nature* **2012**, *490*, 192 – 200.
[3] a) K. S. Novoselov, A. K. Geim, S. V. Morozov, D. Jiang, M. I. Katsnelson, I. V. Grigorieva, S. V. Dubonos, A. A. Firsov, *Nature* **2005**, *438*, 197 – 200; b) R. M. Westervelt, *Science* **2008**, *320*, 324 – 325.
[4] a) F. Schedin, A. K. Geim, S. V. Morozov, E. W. Hill, P. Blake, M. I. Katsnelson, K. S. Novoselov, *Nat. Mater.* **2007**, *6*, 652 – 655; b) V. Dua, S. P. Surwade, S. Ammu, S. R. Agnihotra, S. Jain, K. E. Roberts, S. Park, R. S. Ruoff, S. K. Manohar, *Angew. Chem.* **2010**, *122*, 2200 – 2203; *Angew. Chem. Int. Ed.* **2010**, *49*, 2154 – 2157.
[5] a) M. Pumera, *Energy Environ. Sci.* **2011**, *4*, 668 – 674; b) Y. Q. Sun, Q. O. Wu, G. Q. Shi, *Energy Environ. Sci.* **2011**, *4*, 1113 – 1132.
[6] M. D. Stoller, S. J. Park, Y. W. Zhu, J. H. An, R. S. Ruoff, *Nano Lett.* **2008**, *8*, 3498 – 3502.
[7] G. M. Scheuermann, L. Rumi, P. Steurer, W. Bannwarth, R. Mülhaupt, *J. Am. Chem. Soc.* **2009**, *131*, 8262 – 8270.
[8] W. R. Yang, K. R. Ratinac, S. P. Ringer, P. Thordarson, J. J. Gooding, F. Braet, *Angew. Chem.* **2010**, *122*, 2160 – 2185; *Angew. Chem. Int. Ed.* **2010**, *49*, 2114 – 2138.
[9] K. S. Novoselov, D. Jiang, F. Schedin, T. J. Booth, V. V. Khotkevich, S. V. Morozov, A. K. Geim, *Proc. Natl. Acad. Sci. USA* **2005**, *102*, 10451 – 10453.
[10] a) K. S. Kim, Y. Zhao, H. Jang, S. Y. Lee, J. M. Kim, K. S. Kim, J. H. Ahn, P. Kim, J. Y. Choi, B. H. Hong, *Nature* **2009**, *457*, 706 – 710; b) X. S. Li, W. W. Cai, J. H. An, S. Kim, J. Nah, D. X. Yang, R. Piner, A. Velamakanni, I. Jung, E. Tutuc, S. K. Banerjee, L. Colombo, R. S. Ruoff, *Science* **2009**, *324*, 1312 – 1314.
[11] C. Berger, Z. M. Song, X. B. Li, X. S. Wu, N. Brown, C. Naud, D. Mayou, T. B. Li, J. Hass, A. N. Marchenkov, E. H. Conrad, P. N. First, W. A. de Heer, *Science* **2006**, *312*, 1191 – 1196.
[12] V. León, M. Quintana, M. A. Herrero, J. L. G. Fierro, A. de La Hoz, M. Prato, E. Vázquez, *Chem. Commun.* **2011**, *47*, 10936 – 10938.
[13] L. Chen, Y. Hernandez, X. L. Feng, K. Müllen, *Angew. Chem.* **2012**, *124*, 7758 – 7773; *Angew. Chem. Int. Ed.* **2012**, *51*, 7640 – 7654.
[14] a) J. M. Mativetsky, A. Liscio, E. Treossi, E. Orgiu, A. Zanelli, P. Samorì, V. Palermo, *J. Am. Chem. Soc.* **2011**, *133*, 14320 – 14326; b) F. J. Tölle, M. Fabritius, R. Mülhaupt, *Adv. Funct. Mater.* **2012**, *22*, 1136 – 1144.
[15] J. N. Coleman, *Acc. Chem. Res.* **2013**, *46*, 14 – 22.
[16] A. Ciesielski, P. Samorì, *Chem. Soc. Rev.* **2014**, *43*, 381 – 398.
[17] a) Y. Hernandez, V. Nicolosi, M. Lotya, F. M. Blighe, Z. Sun, S. De, I. T. McGovern, B. Holland, M. Byrne, Y. K. Gun′Ko, J. J. Boland, P. Niraj, G. Duesberg, S. Krishnamurthy, R. Goodhue, J. Hutchison, V. Scardaci, A. C. Ferrari, J. N. Coleman, *Nat. Nanotechnol.* **2008**, *3*, 563 – 568; b) H. Kim, C. Mattevi, H. J. Kim, A. Mittal, K. A. Mkhoyan, R. E. Riman, M. Chhowalla, *Nanoscale* **2013**, *5*, 12365 – 12374.
[18] a) C. E. Hamilton, J. R. Lomeda, Z. Sun, J. M. Tour, A. R. Barron, *Nano Lett.* **2009**, *9*, 3460 – 3462; b) M. El Gemayel, S. Haar, F. Liscio, A. Schlierf, G. Melinte, S. Milita, O. Ersen, A. Ciesielski, V. Palermo, P. Samorì, *Adv. Mater.* **2014**, DOI: 10.1002/adma.201400895.
[19] X. Li, G. Zhang, X. Bai, X. Sun, X. Wang, E. Wang, H. Dai, *Nat. Nanotechnol.* **2008**, *3*, 538 – 542.
[20] A. B. Bourlinos, V. Georgakilas, R. Zboril, T. A. Steriotis, A. K. Stubos, *Small* **2009**, *5*, 1841 – 1845.
[21] C. Schafhaeutl, *J. Prakt. Chem.* **1840**, *19*, 159 – 174.
[22] a) M. S. Dresselhaus, G. Dresselhaus, *Adv. Phys.* **2002**, *51*, 1 – 186; b) X. Dong, Y. Shi, Y. Zhao, D. Chen, J. Ye, Y. Yao, F. Gao, Z. Ni, T. Yu, Z. Shen, *Phys. Rev. Lett.* **2009**, *102*, 135501; c) J. Geng, B. S. Kong, S. B. Yang, H. T. Jung, *Chem. Commun.* **2010**, *46*, 5091 – 5093.
[23] a) M. Lotya, Y. Hernandez, P. J. King, R. J. Smith, V. Nicolosi, L. S. Karlsson, F. M. Blighe, S. De, Z. M. Wang, I. T. McGovern, G. S. Duesberg, J. N. Coleman, *J. Am. Chem. Soc.* **2009**, *131*, 3611 – 3620; b) A. A. Green, M. C. Hersam, *Nano Lett.* **2009**, *9*, 4031 – 4036.
[24] a) X. H. An, T. J. Simmons, R. Shah, C. Wolfe, K. M. Lewis, M. Washington, S. K. Nayak, S. Talapatra, S. Kar, *Nano Lett.* **2010**, *10*, 4295 – 4301; b) X. Y. Zhang, A. C. Coleman, N. Katsonis, W. R. Browne, B. J. van Wees, B. L. Feringa, *Chem. Commun.* **2010**, *46*, 7539 – 7541; c) A. Schlierf, H. Yang, E. Gebremedhn, E. Treossi, L. Ortolani, L. Chen, A. Minoia, V. Morandi, P. Samorì, C. Casiraghi, D. Beljonne, V. Palermo, *Nanoscale* **2013**, *5*, 4205 – 4216; d) H. Yang, Y. Hernandez, A. Schlierf, A. Felten, A. Eckmann, S. Johal, P. Louette, J. J. Pireaux, X. Feng, K. Müllen, V. Palermo, C. Casiraghi, *Carbon* **2013**, *53*, 357 – 365.
[25] S. Sampath, A. N. Basuray, K. J. Hartlieb, T. Aytun, S. I. Stupp, J. F. Stoddart, *Adv. Mater.* **2013**, *25*, 2740 – 2745.
[26] a) A. B. Bourlinos, V. Georgakilas, R. Zboril, T. A. Steriotis, A. K. Stubos, C. Trapalis, *Solid State Commun.* **2009**, *149*, 2172 – 2176; b) F. Liu, J. Y. Choi, T. S. Seo, *Chem. Commun.* **2010**, *46*, 2844 – 2846.
[27] L. L. Chua, J. Zaumseil, J. F. Chang, E. C. W. Ou, P. K. H. Ho, H. Sirringhaus, R. H. Friend, *Nature* **2005**, *434*, 194 – 199.
[28] a) Y. T. Liang, M. C. Hersam, *J. Am. Chem. Soc.* **2010**, *132*, 17661 – 17663; b) L. Xu, J.-W. McGraw, F. Gao, M. Grundy, Z. Ye, Z. Gu, J. L. Shepherd, *J. Phys. Chem. C* **2013**, *117*, 10730 – 10742.
[29] a) S. De Feyter, F. C. De Schryver, *Chem. Soc. Rev.* **2003**, *32*, 139 – 150; b) A. Ciesielski, C.-A. Palma, M. Bonini, P. Samorì, *Adv. Mater.* **2010**, *22*, 3506 – 3520; c) K. S. Mali, J. Adisoejoso, E. Ghijsens, I. De Cat, S. De Feyter, *Acc. Chem. Res.* **2012**, *45*, 1309 – 1320.
[30] A. Ciesielski, P. Samorì, *Nanoscale* **2011**, *3*, 1397 – 1410.
[31] J. P. Rabe, S. Buchholz, *Science* **1991**, *253*, 424 – 427.

[32] a) M. Hibino, A. Sumi, H. Tsuchiya, I. Hatta, *J. Phys. Chem. B* **1998**, *102*, 4544 – 4547; b) L. K. Thomas, A. Kühnle, S. Rode, U. Beginn, M. Reichling, *J. Phys. Chem. C* **2010**, *114*, 18919 – 18924.
[33] U. Khan, A. O'Neill, H. Porwal, P. May, K. Nawaz, J. N. Coleman, *Carbon* **2012**, *50*, 470 – 475.
[34] C. A. Palma, M. Bonini, A. Llanes-Pallas, T. Breiner, M. Prato, D. Bonifazi, P. Samori, *Chem. Commun.* **2008**, 5289 – 5291.
[35] a) A. C. Ferrari, J. C. Meyer, V. Scardaci, C. Casiraghi, M. Lazzeri, F. Mauri, S. Piscanec, D. Jiang, K. S. Novoselov, S. Roth, A. K. Geim, *Phys. Rev. Lett.* **2006**, *97*, 187401; b) C. Casiraghi in *Spectroscopic Properties of Inorganic and Organometallic Compounds*: *Techniques*, *Materials and Applications*, *Vol. 43*, The Royal Society of Chemistry, Cambridge, **2012**, pp. 29 – 56.
[36] M. Lazzeri, S. Piscanec, F. Mauri, A. C. Ferrari, J. Robertson, *Phys. Rev. B* **2006**, *73*, 155426.
[37] C. Casiraghi, A. Hartschuh, H. Qian, S. Piscanec, C. Georgi, A. Fasoli, K. S. Novoselov, D. M. Basko, A. C. Ferrari, *Nano Lett.* **2009**, *9*, 1433 – 1441.
[38] A. Eckmann, A. Felten, I. Verzhbitskiy, R. Davey, C. Casiraghi, *Phys. Rev. B* **2013**, *88*, 035426.

